

Superplastic-Like Flow in Nanocrystalline ZrO₂-Spinel Two Phase Composite

K. Morita, B.-N. Kim, H. Yoshida and K. Hiraga

National Institute for Materials Science, 1-2-1 Sengen, Tsukuba, Ibaraki 305-0047

Fax: +81-29-859-2501, e-mail: MORITA.Koji@nims.go.jp

The effect of nanocrystallization on superplastic flow was examined in ZrO₂-30vol% spinel composite. As compared with the superplasticity of submicro-grain composite, the nanocrystallization can increase the strain rate by one order of magnitude or lower the deforming temperature by about 100 K. Irrespective of the lowered flow stress, however, the maximum tensile elongation to failure of nanocrystalline composite is about 100%, which is several times lower than that of submicrom-grain composite. The limited tensile elongation in nanocrystalline composite can be ascribed mainly to accelerating cavity damage accumulation.

Keywords: ZrO₂, nano-composite, high-energy ball-milling, superplasticity

1. INTRODUCTION

Recently, we have attained high-strain-rate superplasticity (HSRS) in fine particle dispersed ZrO₂ composites [1-4]. For Al₂O₃-spinel-ZrO₂ tri-phase composite [1,2], for example, a large tensile elongation to failure, ϵ_B , excess of 390% was attained even at a remarkable high strain rate of $\approx 1.0 \text{ s}^{-1}$ and at 1923 K. For industrial forming applications, however, further improvement of superplastic properties is required: for example, low deforming temperature, high available strain rate and large tensile elongation.

For this purpose, reducing the grain size is expected to be one of the promising ways because strain rate and deforming temperature are related closely to grain size as characterized by the following empirical creep equation:

$$\dot{\epsilon} = A\sigma^{1/m}d^p\exp(-Q/RT), \quad (1)$$

where $\dot{\epsilon}$ is the steady-state strain rate, σ is the true stress, m is the strain rate sensitivity, d is the grain size, p is the grain size exponent, Q is the apparent activation energy, R is the gas constant, T is the absolute temperature and A is a constant.

With regard to ceramic materials, the effect of nanocrystallization on superplasticity has been studied in monoclinic ZrO₂ [5,6] and yttria-stabilized tetragonal (*t*-) ZrO₂ [7-9]. In the most studies [5-9], however, the flow behavior has been examined only by compression and thereby the experimental data on tension is highly limited. For ceramics, since cavitation due to decohesion of grain boundaries have limited tensile elongation, experimental data in tension is necessary to discuss deformability of

nanocrystalline ceramics.

The present study was therefore performed to examine superplasticity of nanocrystalline ceramics in tension. In this study, we deal with ZrO₂-30vol% MgAl₂O₄ spinel two-phase composite because the composite can attain HSRS at strain rates higher than 10^{-1} s^{-1} even at submicro-grain of 350 nm [3,4].

2. EXPERIMENTAL PROCEDURES

2.1 Materials

Nanocrystalline ZrO₂-30vol% MgAl₂O₄ spinel composite was fabricated by employing high-energy ball-milling and spark-plasma-sintering (SPS) techniques [10]. 3mol%-Y₂O₃-stabilized ZrO₂ powder (TZ-3Y, Tosoh Co., Ltd.) mixed with 30vol% spinel powder (SP-12, Iwatani Co. Ltd.) was milled with a planetary ball-milling machine for 400 h in ethanol using ZrO₂ ball media and container. The milled powders were consolidated with a SPS machine (Sumitomo Coal Mining Co., Japan) under vacuum condition. By applying a load of 70 MPa, the milled powders were rapidly heated up to 1573 K at a heating rate of about 100 °C/min and then held at the temperature for 5 min.

2.2 Microstructural Characterization.

The microstructural characterizations were conducted by TEM and SEM. For TEM observation, thin sheets with a thickness of about 500 μm were cut from the SPSed materials with a low-speed diamond cutter, mechanically polished to about 100 μm in thickness and further thinned with an Ar ion-milling machine. For SEM

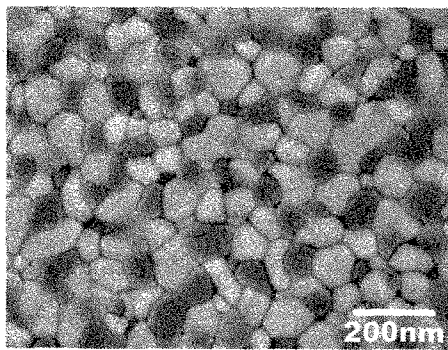


Fig. 1 SEM image of ZrO_2 -30vol% spinel composite as-SPSed at 1573 K [12].

observation, the surface of the specimens were mechanically polished and thermally etched at 1473 K for 10 min, at which grain growth is negligible. The average grain size, d , was determined as 1.56 times of the average intercept lengths of grains in SEM micrographs [11].

2.3 Tensile Test.

Superplasticity was examined by constant displacement-rate tensile tests under vacuum using an Instron-type tensile machine. From the SPSed circular disks, dog-bone-shaped flat tensile specimens were machined with gauge portions of 2.3×10 mm. The tensile tests were conducted at 1473-1673 K and at initial strain rates of $\dot{\epsilon}_0 \approx 1.7 \times 10^{-4} - 0.1 \text{ s}^{-1}$.

3. EXPERIMENTAL RESULTS

3.1 Sintered Microstructure

Figure 1 shows typical SEM images of ZrO_2 -30vol% spinel composite [12]. The light and dark contrast corresponds to the ZrO_2 and spinel grains, respectively. By using SPS process, dense and nanocrystalline ZrO_2 -spinel composite with relative

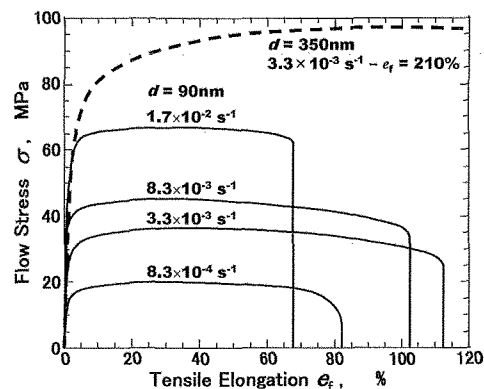


Fig. 2 True stress - strain curves for 30vol% spinel dispersed ZrO_2 composite deformed at 1623 K [12].

density higher than 98 % can successfully be fabricated. The average grain size is about 96 nm. For the nanocrystalline composite, the spinel particles disperse homogenously among ZrO_2 matrix and no agglomeration was found.

The microstructural examination by high-resolution TEM showed that the lattice fringes of each grain intersect at the boundary without any second phases and no amorphous phase was found along grain boundaries and at multiple-grain junctions. XRD profile can be indexed from the tetragonal (t -) ZrO_2 and spinel phases, but no monoclinic and cubic ZrO_2 phases was detected.

3.2 Superplastic Flow behavior

Figures 2 show stress-strain curves of nanocrystalline ZrO_2 -spinel composite tested at 1623 K and at $\dot{\epsilon}_0 \approx 1.7 \times 10^{-2} - 8.3 \times 10^{-4} \text{ s}^{-1}$ [12]. For comparison, a flow curve of submicro-grain composite with $d = 350$ nm is also shown by broken-line. It is apparent from the flow curves that the flow stress σ can effectively be lowered to 1/2-1/3 due to nanocrystallization. In general,

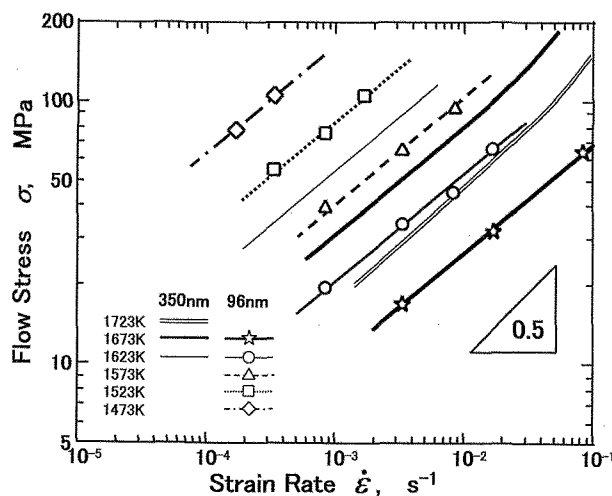


Fig. 3 Flow stresses σ of nanocrystalline and submicrom-grain composites plotted as a function of strain rate $\dot{\epsilon}$ [12].

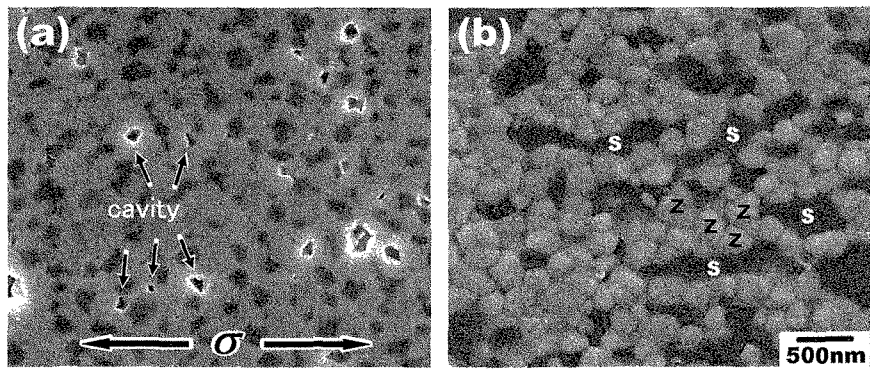


Fig. 4 Typical microstructure of (a) nanocrystalline and (b) submicro-grain composites after deformation at 1623 K and at $\dot{\epsilon} = 8.3 \times 10^{-4} \text{ s}^{-1}$; (a) $\epsilon_f \approx 80\%$ and (b) $\epsilon_f \approx 100\%$ [12].

tensile elongation to failure e_f tends to increase with decreasing flow stress as noted by Kim *et al.* [13]. In the present composites, however, the maximum e_f -value is smaller than 120%, which is several times smaller as compared with those of submicro-grain materials.

The flow stress σ – strain rate $\dot{\epsilon}$ relationship of nanocrystalline composite is shown in Fig. 3. [12]. For comparison, the data for submicro-grain composite are also plotted [14]. The σ – $\dot{\epsilon}$ relationship shows that reducing the grain size to nanocrystalline ranges can enhance strain rate of one order of magnitude or decreases deformable temperature of the order of 100 K.

The m -value evaluated from the σ - $\dot{\epsilon}$ relationship takes about 0.45, which is consistent with a typical value of 0.5 for superplastic flow [15]. On the other hand, the Q -value evaluated at 60 MPa takes ≈ 690 kJ/mol, which is slightly higher than ≈ 560 kJ/mol reported in submicro-grain ZrO_2 -spinel composite [14]. The increase in the Q -value due to nanocrystallization was also reported in monolithic tetragonal (t -) ZrO_2 . For nanocrystalline t - ZrO_2 , the Q -value takes ≈ 630 kJ/mol [8], whereas for submicro-grain t - ZrO_2 , it takes ≈ 580 kJ/mol [16,17], which has been related to lattice diffusion of cations.

3.4 Deformed Microstructure

Figure 4 shows an example of deformed microstructure of nanocrystalline and submicro-grain ZrO_2 -spinel composites [12]. The SEM image exhibits two characteristic microstructures, which depend strongly on grain size.

First, for submicro-grain composite in Fig. 4(b), cavities can be rarely found, whereas for nanocrystalline composite Fig. 4(a), many fine cavities are observed to form at multiple grain junctions. Superplastic properties have often been associated with the flow stress level [13]

and intergranular cavitation [18]. For nanocrystalline composite, the accelerating cavity damage accumulation inhibits tensile elongation though the flow stress can be lowered due to nanocrystallization.

Second, for submicro-grain composite, spinel phase tends to elongate along tensile direction (horizontal), whereas for nanocrystalline composite, it retain almost the initial equiaxed shape as reported in the most superplastic ceramics [15]. For submicro-grain composite, the elongation of spinel phase is typical microstructural feature deformed at high-strain-rates [14]. The microstructural feature suggests that the deformable spinel phase can contribute to the enhanced accommodation of the stress concentrations exerted by GBS [14]. For nanocrystalline composite, however, the microstructural examination showing equiaxed grain shape suggests that, in contrast to submicro-grain composite, the spinel phase may not contribute to the accommodation process of grain boundary sliding (GBS).

4. DISCUSSION

The flow mechanism has often been characterized by creep parameters (m , Q and p) determined by Eq. (1). The σ - $\dot{\epsilon}$ relationship in Fig. 3 indicates that, irrespective of grain size, the m -value takes about 0.5, which is a typical value for superplastic flow [15]. For fine-grained ceramics characterized by $m \approx 0.5$, GBS process has generally been regarded as the dominant flow mechanism. It is therefore reasonable to explain that the deformation of the nanocrystalline composite also takes place primarily through GBS. Thus, the lowered flow stress would not result from the change in the flow mechanism but result from the decreases in grain size as expected from Eq. (1).

For the present nanocrystalline composite, the activation energy takes slightly higher value of $Q \approx 690$

kJ/mol as compared with that of submicro-grain composite [12]. During deformation by GBS in a polycrystalline matrix, stress concentrations must be exerted around multiple grain boundary junctions and ledges. Thus, for continuous deformation by GBS, a concomitant accommodation of the stress concentrations is required through diffusion processes along the boundaries and/or through grains or by plastic deformation. The increase in the Q -value suggests that, for ZrO_2 ceramics, rate controlling process of superplastic flow may change due to nanocrystallization though the deformation takes place dominantly by GBS irrespective of grain size.

The microstructural feature suggests that, in contrast to submicro-grain composite, the spinel phase may not contribute to the accommodation process of GBS in nanocrystalline composite. Although another examination is necessary to discuss detailed flow mechanism, the difference in the deformed microstructure may also be related to the change in the Q -value and hence result in the limited tensile elongation in the nanocrystalline composite.

5. SUMMARY

The effect of nanocrystallization on superplasticity was examined in ZrO_2 -30vol% spinel two phase composite. The nanocrystallization can enhance strain rate of one order of magnitude or decreases deforming temperature of the order of 100 K. However, the tensile elongation to failure e_f of nanocrystalline composite is lower than that of submicrom-grain composite. The limited tensile elongation in nanocrystalline composite may be ascribed mainly due to accelerating cavity damage accumulation.

The flow behavior of nanocrystalline composite can be characterized by $m \approx 0.5$ and $Q \approx 690$ kJ/mol. The $m \approx 0.5$ suggests that the flow behavior can be ascribed to GBS mechanism as well as submicro-grain composite. The change in accommodation of GBS may cause the limited tensile elongation in the nanocrystalline composite.

ACKNOWLEDGEMENTS

The authors are grateful to the Mitsubishi Foundation for supporting a part of the present work.

REFERENCES

- [1] B.-N. Kim, K. Hiraga, K. Morita, Y. Sakka, *Nature* **413**, 288 (2001).
- [2] B.-N. Kim, K. Hiraga, K. Morita, Y. Sakka, T. Yamada, *Scripta Mater.*, **47**, 775 (2002).
- [3] K. Morita, K. Hiraga, Y. Sakka, *J. Am. Ceram. Soc.*, **85**, 1900 (2002).
- [4] K. Morita, K. Hiraga, B.-N. Kim, Y. Sakka, *Mater. Trans.*, **45**, 2073 (2004).
- [5] M. J. Roddy, W. R. Cannon, G. Skandan, H. Hahn, *J. Eur. Ceram. Soc.* **22** (2002) 2657.
- [6] M. Yoshida, Y. Shinoda, T. Akatsu, F. Wakai, *J. Am. Ceram. Soc.* **85** (2002) 2834.
- [7] M. Ciftcioglu, M. J. Mayo, *Mat. Res. Soc. Symp. Proc.* **196** (1990) 77.
- [8] F. Gutiérrez-Mora, A. Domínguez-Rodoriguez, M. Jiménez-Melendo, *J. Euro. Ceram. Soc.* **22** (2002) 2615.
- [9] R. Chaim, R. Ramamoorthy, A. Goldstein, I. Eldror, A. Gurman, *J. Euro. Ceram. Soc.* **23** (2003) 647.
- [10] K. Morita, K. Hiraga, B.-N. Kim, H. Yoshida, Y. Sakka, *Scripta Mater.*, **53**, 1007 (2005).
- [11] J.C. Wurst, J.A. Nelson, *J. Am. Ceram. Soc.*, **55**, 109 (1972).
- [12] K. Morita, K. Hiraga, B.-N. Kim and H. Yoshida, to be submitted.
- [13] W.J. Kim, J. Wadsworth, O.D. Sherby, *Acta Mater.*, **39**, 199 (1991).
- [14] K. Morita, K. Hiraga and B.-N. Kim, to be submitted.
- [15] T.G. Nieh, J. Wadsworth, O.D. Sherby, *Superplasticity in Metals and Ceramics*. Cambridge University Press, United Kingdom, 1997.
- [16] M. Jiménez-Melendo, A. Domínguez-Rodoriguez, A. Bravo-León, *J. Am. Ceram. Soc.*, **81**, 2761 (1998).
- [17] K. Morita, K. Hiraga, *Acta Mater.*, **50**, 1075 (2002).
- [18] K. Hiraga, K. Nakano, T.S. Suzuki, and Y. Sakka, *J. Am. Ceram. Soc.*, **85**, 2763 (2002).

(Received December 10, 2006; Accepted May 11, 2007)